Acta Neuropathologica (2019) 138:783–793
https://doi.org/10.1007/s00401-019-02028-6

ORIGINAL PAPER

Increased prevalence of granulovacuolar degeneration in C9orf72 mutation

Yuichi Riku[1,6] · Charles Duyckaerts[1,2,3] · Susana Boluda[1,3] · Isabelle Plu[1,2] · Isabelle Le Ber[3,4] · Stéphanie Millecamps[3] · François Salachas[5] · Brainbank NeuroCEB Neuropathology Network · Mari Yoshida[7] · Takashi Ando[6] · Masahisa Katsuno[6] · Gen Sobue[8] · Danielle Seilhean[1,2,3]

Received: 8 February 2019 / Revised: 20 May 2019 / Accepted: 21 May 2019 / Published online: 29 May 2019

Abstract

Granulovacuolar degeneration (GVD) is usually found in Alzheimer's disease (AD) cases or in elderly individuals. Its severity correlates positively with the density of neurofibrillary tangles (NFTs). Mechanisms underlying GVD formation are unknown. We assessed the prevalence and distribution of GVD in cases with TDP-43-related frontotemporal lobar degeneration (FTLD-TDP) and amyotrophic lateral sclerosis (ALS-TDP). Consecutively autopsied cases with FTLD/ALS-TDP and C9orf72 mutations (FTLD/ALS-C9; $N=29$), cases with FTLD/ALS-TDP without C9orf72 mutations (FTLD/ALS-nonC9; $N=46$), and age-matched healthy controls ($N=40$) were studied. The prevalence of GVD was significantly higher in the FTLD/ALS-C9 cases (26/29 cases) than in the FTLD/ALS-nonC9 cases (15/46 cases; Fisher exact test; $p<2\times10^{-6}$) or in the control group (12/40 individuals; $p<1\times10^{-6}$). Average Braak stages and ages of death were not significantly different among the groups. The CA2 sector was most frequently affected in the FTLD/ALS-C9 group, whereas the CA1/subiculum was the most vulnerable area in the other groups. Extension of GVD correlated with the clinical duration of the disease in the FTLD/ALS-C9 cases but not in the FTLD/ALS-nonC9 cases. The GVD-containing neurons frequently had dipeptide repeat (DPR) protein inclusions. GVD granules labeled with antibodies directed against charged multivesicular body protein 2B or casein kinase 1δ were attached to DPR inclusions within GVD. Our results suggest that development of GVD and DPR inclusions is related to common pathogenic mechanisms and that GVD is not only associated with NFTs seen in AD cases or aging individuals.

Keywords ALS · C9orf72 · Dipeptide repeat · FTLD · Granulovacuolar degeneration · TDP-43

The members of the NeuroCEB Brainbank Neuropathology Network are listed in Acknowledgements.

✉ Charles Duyckaerts
charles.duyckaerts@aphp.fr

[1] Raymond Escourolle Neuropathology Department, Groupe Hospitalier Pitié-Salpêtrière Charles Foix, AP-HP, 75651 Cedex 13 Paris, France

[2] Faculty of Medicine, Sorbonne University, 75013 Paris, France

[3] Institut du Cerveau et de la Moelle épinière (ICM), Inserm U 1127, CNRS UMR7225, Sorbonne University, 75013 Paris, France

[4] National Reference Center for Rare or Early Dementias, Institute of Memory and Alzheimer's Disease (IM2A), Center of Excellence of Neurodegenerative Disease (CoEN), Department of Neurology, Groupe Hospitalier Pitié-Salpêtrière Charles Foix AP-HP, 75013 Paris, France

[5] Reference Center for ALS, Department of Neurology, Groupe Hospitalier Pitié-Salpêtrière Charles Foix, AP-HP, 75013 Paris, France

[6] Department of Neurology, Nagoya University, Nagoya, Japan

[7] Institute for Medical Science of Aging, Aichi Medical University, Aichi, Japan

[8] Graduate School of Medicine, Nagoya University, Nagoya, Japan

Introduction

TAR DNA-binding protein 43 kDa (TDP-43) is a major component of aggregated proteins observed in cases with frontotemporal lobar degeneration (FTLD) and amyotrophic lateral sclerosis (ALS-TDP) [23]. ALS-TDP and FTLD-TDP can co-occur, a condition known as frontotemporal dementia with motor neuron disease (FTD-MND) or ALS with dementia (ALS-D) [12]. FTLD-TDP and ALS-TDP belong to a continuous spectrum of diseases grouped under the term 'TDP-43 proteinopathy' that variably involve multiple systems of neural connection [10, 26–28].

The mutation of the C9orf72 gene was identified as the most common genetic cause of familial FTLD/ALS-TDP (FTLD/ALS-C9) [8, 21]. In this mutation, an intronic hexanucleotide (GGGGCC) expansion leads to non-ATG mediated sense and antisense translation, which results in the formation of dipeptide repeat (DPR) proteins [1, 20]. Inclusions of poly-GA, poly-GP, and poly-GR, which are products of sense translation, are more abundant than those of poly-PA or poly-PR derived from antisense translation [15]. Immunohistochemically, the DPR inclusions are p62/ubiquitin-positive but TDP-43-negative [1]. Recent studies have revealed key roles of C9orf72 genes for the autophagy system [32] and the endosome system [31]. Neurotoxicity of DPR inclusions [17, 37], TDP-43 inclusions [7], and repeat RNA have also been reported in that mutation [33].

In this study, we analyzed the prevalence of granulovacuolar degeneration (GVD) in FTLD/ALS-TDP cases. In H&E-stained specimens, GVD is composed of basophilic granules in vacuoles. They are usually found in the pyramidal neurons of the hippocampus in AD cases [14, 35]. The prevalence of GVD strongly correlates with the density of neurofibrillary tangles (NFTs). It can arise in non-demented elderly individuals or in cases with tauopathy other than AD [14, 35]. GVD granules contain miscellaneous proteins, including hyperphosphorylated tau (pTau) and phosphorylated TDP-43 (pTDP-43) [13, 38]. GVD is usually not found in neurons bearing NFTs or cytoplasmic inclusion of TDP-43 [13, 38]. Recent studies revealed that GVD granules structurally resemble autophagic organelles and abundantly aggregate charged multivesicular body protein 2B (CHMP2B), an endosome-related protein [9, 39]. The prevalence of GVD is unknown among FTLD/ALS-TDP, and mechanisms of GVD formation remain to be elucidated. We assessed GVD among consecutively autopsied cases with FTLD/ALS-C9 ($n=29$), cases with C9orf72 mutation-negative FTLD/ALS-TDP ($n=46$), and controls without neurological disorders ($n=40$).

Materials and methods

Genetic analysis

The C9ORF72 repeat was analyzed in all cases with FTLD or ALS using a repeat-primed PCR amplification as we described previously [19]. The assay was completed by a classical fluorescent fragment length analysis allowing the detection of non-expanded C9orf72 alleles. These analyses were repeated twice for each patient to ensure reproducibility of the results. DNA of some homozygous individuals was sequenced to precisely correlate the number of base pairs in the fluorescent assay with the number of GGGGCC repeats. Cases with GGGGCC repeat numbers larger than 50 were included in the C9orf72-related FTLD/ALS (FTLD/ALS-C9) group. The other cases were classified to the non-C9-orf72-related FTLD/ALS (FTLD/ALS-nonC9) group.

Subjects

Signed informed consent for autopsy and genetic analysis was obtained in all cases from the patients themselves or from the patients' family members. Eighty-seven cases with FTLD/ALS-TDP who were consecutively autopsied between January 1998 and December 2016 at Raymond Escourolle Neuropathology Laboratory [30, 34] were studied. In 33 individuals, an expansion of GGGGCC repeat in C9orf72 gene had been identified (FTLD/ALS-C9); in 54 individuals, no GGGGCC expansion of C9orf72 gene was detected (FTLD/ALS-nonC9). Cases with comorbid AD pathology that corresponded to Braak NFT stage IV or higher [2] or Thal amyloid phase 3 or higher [36] were excluded from the study. pTau-positive GVD granules were not taken into account in Braak NFT staging. Cases in the limbic or neocortical stage of dementia with Lewy bodies [18] or with argyrophilic grain disease (AGD) at Saito's stage II or above [29] were also excluded. After exclusion of inadequate cases, 29 cases with FTLD/ALS-C9 and 46 cases with FTLD/ALS-nonC9 were included to the study. Forty age-matched controls without any neurological diseases (9 females and 31 males) were compared to the FTLD/ALS-TDP cases. Causes of death included carcinoma/hematologic neoplasms ($N=14$), cardiovascular diseases ($N=8$), infections ($N=4$), enteral hemorrhage ($N=3$), and other conditions ($N=11$; collagen diseases, diabetes mellitus, liver cirrhosis, and sudden death due to unknown causes). The demographic characteristics of the subjects under study are summarized in Table 1. Average Braak NFT stages and ages of death did not differ among the three groups. Two cases in the ALS-C9 subgroup, one in the ALS-nonC9 subgroup, and one in the control group had AGD Saito's grade I.

Table 1 Clinical and pathological data

	FTLD/ALS-C9	FTLD/ALS-nonC9	Controls	*p* value
N (gender)	29 (7F/22M)	46 (13F/33M)	40 (9F/31M)	0.8 (F/M)[a]
Age at death (average)	60.1 ± 9.6 (42–72)	62.5 ± 9.7 (40–75)	61.2 ± 7.6 (47–75)	0.4[b]
Duration (month, median)	48 (6–192)	37 (8–136)	–	0.5[c]
Clinical subgroups				
FTD (without ALS)	5 (1F/4M)	2 (1F/1M)	–	
FTD (with ALS)	14 (3F/11M)	14 (4F/10M)	–	
ALS	10 (3F/7M)	30 (8F/22M)	–	
Family history	93.1% (27/29)	0.0% (0/46)	–	< 0.001[a]
Brain weight (average)	1266.4 ± 183.9	1372.4 ± 173.2	1407.4 ± 130.3	< 0.05[b]
PMD (median)	24.0 (9–72)	27.5 (2–84)	23 (3–72)	0.2[b]
TDP-43 subtype of FTLD				
Type A	6	7	–	0.5[a]
Type B	13	8	–	0.3[a]
Type C	0	1	–	0.5[a]
Braak NFT stage (average)	0.97 ± 0.94	0.74 ± 0.80	1.00 ± 0.99	0.5[b]
Thal amyloid phase (average)	0.14 ± 0.35	0.24 ± 0.53	0.25 ± 0.54	0.9[b]

Clinical and pathological data of the three groups of cases studied: FTLD/ALS-C9: fronto-temporal lobar degeneration or amyotrophic lateral sclerosis, diversely associated, with C9orf72 mutation. FTLD/ALS-non C9: fronto-temporal lobar degeneration or amyotrophic lateral sclerosis, diversely associated, without C9orf72 mutations

ALS amyotrophic lateral sclerosis; *FTD* frontotemporal dementia; *FTLD* frontotemporal lobar degeneration; *NFT* neurofibrillary tangle; and *PMD* post-mortem delay

[a]Fisher's exact test. [b]Kruskal–Wallis test. [c]Mann–Whitney *U* test

Clinical analysis

The clinical review of the cases was retrospective. Gender, age of death, duration of symptomatic disease, subtype of dementia, family history, brain weight, and post-mortem delay were recorded. Onset of disease was defined as the first awareness of dementia symptoms or muscle weakness by patients or caregivers. The occurrence of ALS, dementia or both within two generations among first to fourth degree relatives was taken as evidence of a family history. Two clinical subgroups, FTD and non-demented ALS, were recognized among the cases. The FTD cases, with or without ALS, were defined as those who showed behavioral variant FTD (bvFTD) or primary progressive aphasia [22] and demonstrated neuronal TDP-43 inclusions in the frontotemporal cortices. The ALS cases were defined as those who presented with ALS in the absence of dementia throughout the course of the disease and in which TDP-43 inclusions were detected in the motor neurons [5]. The FTLD/ALS-C9 group comprised 19 FTD cases (with or without ALS) and 10 pure ALS cases. The FTLD/ALS-nonC9 group comprised 16 FTD cases (with or without ALS) and 30 pure ALS cases (Table 1).

Pathological analysis

The two hemispheres were separated immediately after removal. One hemisphere, randomly left or right, was fixed in 4% neutral-buffered formalin for at least 2 months. Frozen samples were collected from the other hemisphere. The fixed hemisphere was cut at a level of the mammillary bodies, and 10-mm-thick coronal sections were systematically prepared. The tissues were embedded in paraffin, and 5-µm-thick sections were routinely stained with hematoxylin–eosin (H&E) and luxol fast blue. The primary antibodies are listed in Table 2. The slides were immunostained with the Benchmark Ultra or XT (Roche-Ventana) automated slide staining system according to the manufacturer instructions.

Evaluation of GVD

GVD was defined as an accumulation of large membrane-bound vacuoles with a central granule. Single and isolated vacuoles with a granule were excluded. GVD was graded after H&E staining and anti-pTDP-43 immunohistochemistry using the GVD staging system proposed by Thal et al. [35]. Each stage was defined as follows: stage 0, no GVD;

Table 2 Primary antibodies used in this study

Specificity	Clone	Host species	Concentration	Company
Anti-α-synuclein	KM51	Mouse, monoclonal	1:10	Novocastra, Newcastle, UK
Anti-β-amyloid	6F3D	Mouse, monoclonal	1:100	Dako, Glostrup, Denmark
Anti-CHMP2B		Rabbit, polyclonal	1:500	Abcam, Cambridge, MA
Anti-CK1δ	AF12G4	Mouse, monoclonal	1:500	Abcam, Cambridge, MA
Anti-glial fibrillary acidic protein		Rabbit, polyclonal	1:1000	Dako, Glostrup, Denmark
Anti-p62	3/p62 LCK ligand	Mouse, monoclonal	1:500	BD Biosciences, Franklin Lakes, NJ
Anti-phosphorylated tau	AT-8	Mouse, monoclonal	1:500	ThermoScientific, Waltham, MA
Anti-phosphorylated TDP43	pS409/410-2	Rabbit, polyclonal	1:5000	Cosmobio, Tokyo, Japan
Anti-poly-GA	5E9	Mouse, monoclonal	1:100	EMD Millipore, Billerica, MA
Anti-poly-GP		Rabbit, polyclonal	1:80	ProteinTech, Chicago IL
Anti-poly-GR		Rabbit, polyclonal	1:80	ProteinTech, Chicago IL
Anti-poly-PA		Rabbit, polyclonal	1:80	ProteinTech, Chicago IL
Anti-poly-PR		Rabbit, polyclonal	1:80	ProteinTech, Chicago IL
Anti-TDP-43		Rabbit, polyclonal	1:2500	ProteinTech, Chicago IL
Anti-ubiquitin	Ubi-1	Mouse, monoclonal	1:250	EMD Millipore, Billerica, MA

stage 1, GVD limited to the subiculum and CA1; stage 2, GVD involving also CA4 and the entorhinal cortex; stage 3, GVD involving also the temporal neocortex; stage 4, GVD pathology reached the amygdala and hypothalamus; and stage 5, GVD also found in neocortical areas and thalamus. The CA sectors were evaluated in a section made at the level of the geniculate body. Interrater reliability (Y.R. and D.S.) for presence or absence of GVD on H&E staining was found to be excellent (kappa = 0.80 for 10 slides).

Immunohistochemistry for DPR inclusions

We immunohistochemically assessed DPR inclusions containing proteins translated from the sense strand (sense DPRi) with antibodies directed against poly-GA, poly-GP, or poly-GR and DPR inclusions containing proteins translated from the antisense strand (anti-sense DPRi) with antibodies directed against poly-PR or poly-PA in the CA sectors of all cases. Sense DPRi were found in all FTLD/ALS-C9 cases and were more abundant than antisense DPRi that were rarely observed in only a subset of those cases (poly PR and poly PA immunopositivity was found in 13 and 8 out of 29 FTLD/ALS-C9 cases, respectively). DPR inclusions were negative in the FTLD/ALS-nonC9 cases and controls (supplementary Figure).

Quantification of coexistence of GVD with DPR inclusions

The prevalence of DPR inclusions among neurons with or without GVD was manually assessed in DPR immunostained sections with hematoxylin counterstaining under a magnification of 400×. Only neurons of which the whole cell body and nucleus were visible within each microscopical field were counted. Three microscopical fields from the CA2 and five from the CA1 sectors were randomly chosen at 100 µm or more intervals to avoid overlapping. GVD and DPR inclusions could coexist in neurons in two ways; DPR inclusions could be located within GVD and were defined as 'colocalized' with GVD; DPR inclusions could be located outside GVD and were defined as 'separated'. Nine cases of the FTLD/ALS-C9 group that showed GVD both in the CA1 and CA2 sectors, and had both sense and antisense DPRi were analyzed in that way.

Subclassification of TDP-43 pathology

For the cases with the FTD phenotype, cortical TDP-43 pathology was morphologically classified into A, B, C, and D types, according to the harmonized criteria [16].

Immunofluorescence

Double immunofluorescence was used to look for colocalization of DPR, phospho Tau (AT8), or pTDP-43 with GVD markers, CHMP2B or CK1δ. Anti-mouse or anti-rabbit secondary antibodies were coupled with Alexa Fluor 488 or 561 (Molecular Probes, Carlsbad, CA, USA). Triple immunofluorescence was also performed to assess colocalization of CHMP2B, CK1δ, and DPR inclusions using the Opal multiplex IHC 4-color kit (PerkinElmer, Waltham, MA, USA). Slides were deparaffinized. Intrinsic peroxidases were inactivated with 0.3% hydrogen peroxide methanol. A solution of 3 mM citrate buffer at pH 6 was used for antigen retrieval. The sections were then washed in PBS-Tween20 (PBST) and incubated in 1% BSA blocking buffer for 20 min. The slides

were incubated with the primary anti-CHMP2B antibody for 2 h and then, with a peroxidase-labeled secondary antibody for 1 h, followed by amplification with Cy3-labeled tyramide for 10 min. The slides were boiled in 100 °C citrate buffer for 20 min to inactivate the remaining primary antibody. The slides were blocked again with 1% BSA blocking buffer for 20 min and incubated with an anti-poly-GA (mouse) or poly-PR (rabbit) antibody. The sections were incubated with the adequate peroxidase conjugated secondary antibody for 1 h, revealed with FITC-conjugated tyramide. After boiling in 100 °C citrate buffer, the slides were blocked with 1% BSA blocking buffer for 20 min and incubated with the anti-CK1δ mouse antibody for 2 h. The secondary peroxidase-labeled antibody was revealed with Cy5-conjugated tyramide. 4,6-diamidino-2-phenylindole (DAPI) was used to stain nuclei. The labeled sections were observed with a laser confocal microscope (LSM 710, Carl Zeiss, Göttingen, Germany). Images were acquired with the same laser and detection settings.

Statistical analyses

The clinical and pathological findings were compared using the Mann–Whitney *U* test for quantitative variables and the Chi-square test for qualitative variables. When the expected value of the Chi-square test was below five, Fisher's exact test was computed. The Kruskal–Wallis test was used to detect differences in more than three groups. The significance level was set at a p value of 0.05 for comparisons between two groups; the Bonferroni correction was performed for multiple comparisons. All statistical tests were two-sided and were performed using the SPSS 21.0 software program (IBM).

Results

Prevalence and extension of GVD pathology

The prevalence of GVD was not distributed randomly across the FTLD/ALS-C9, FTLD/ALS-nonC9, and control cases (based on H&E, Chi-square = 29.7, degree of freedom = 2, and $p < 0.0001$; based on pTDP-43, Chi-square = 27.3 and $p < 0.0001$). The observed number of FTLD/ALS-C9 cases with GVD ($n = 26$ out of 29 cases with H&E; $n = 27$ out of 29 cases with pTDP-43) was almost twice the expected value (13.3 with H&E and 14.9 with pTDP-43). The comparison of GVD prevalence between the FTLD/ALS-C9 and FTLD/ALS-nonC9 groups was highly significant ($p < 2\times10^{-6}$ with H&E and $p < 3\times10^{-4}$ with pTDP-43), as was the comparison of GVD prevalence in the FTLD/ALS-C9 group and in the control group where GVD were observed in only 12 cases out of 40 individuals ($p < 1\times10^{-6}$ with H&E and $p < 1\times10^{-5}$ with pTDP-43). Comparisons made between the FTD subgroups indicated a higher prevalence of GVD in the FTD-C9 subgroup than in the FTD-nonC9 subgroup ($p < 0.002$ with H&E as well as with pTDP-43, Fisher's exact test). The ALS-C9 subgroup without dementia also showed a higher prevalence of GVD than the ALS-nonC9 subgroup ($p < 0.01$ with H&E and $p = 0.01$ with pTDP-43) (Table 3). Although the prevalence of GVD positively correlated with age at death and NFT stage in all groups, it was significantly higher in the C9 group particularly among younger individuals or at low Braak stages (Tables 4, 5).

GVD in the FTLD/ALS-C9 cases were preferentially located in the CA2 sector, whereas the CA1/subiculum was most vulnerable in the other groups (Fig. 1). In the FTLD/ALS-C9 cases with numerous GVD, GVDs were found in the thalamus or frontal cortex (Fig. 1). Among GVD-positive individuals, the average GVD stage was higher in the FTLD/ALS-C9 group than in the other groups ($p < 0.016$ on H&E and pTDP-43, Mann–Whitney *U* test) (Fig. 1). The spatial extension of GVD in the brain was positively correlated with disease duration in the FTLD/ALS-C9 cases (rho = 0.556 and $p < 0.005$ with H&E; rho = 0.658 and $p < 0.0005$ with pTDP-43, Spearman's rank correlation test); there was no correlation in the FTLD/ALS-nonC9 cases (rho = 0.020 and $p = 0.898$ with H&E; rho = 0.103 and $p = 0.517$ with pTDP-43) (Fig. 1).

Table 3 Prevalence of GVD according to clinical subgroups

	Total	Clinical subgroup	
		FTD (with or without ALS)	ALS
FTLD/ALS-C9			
H&E	90% (26/29)	95% (18/19)	80% (8/10)
pTDP43	93% (27/29)	95% (18/19)	90% (9/10)
FTLD/ALS-nonC9			
H&E	33% (15/46)	43% (7/16)	27% (8/30)
pTDP43	39% (18/46)	43% (7/16)	37% (11/30)
Control			
H&E	30% (12/40)		
pTDP43	35% (14/40)		
p value, C9 vs. nonC9			
H&E	< 0.001*	< 0.002*	< 0.007*
pTDP43	< 0.001*	< 0.002*	< 0.009*
p value, C9 vs. Control			
H&E	< 0.001*		
pTDP43	< 0.001*		

() Indicates number of cases with granulo-vacuolar degeneration/total number of cases

*Fisher's exact test. Significance level < 0.016 after Bonferroni correction

Table 4 Prevalence of GVD according to age at death

	< 60	61–70	70 <
FTLD/ALS-C9			
H&E	80% (8/10)	93% (13/14)	100% (5/5)
pTDP43	90% (9/10)	93% (13/14)	100% (5/5)
FTLD/ALS-nonC9			
H&E	19% (3/16)	33% (6/18)	50% (6/12)
pTDP43	19% (3/16)	33% (6/18)	75% (9/12)
Control			
H&E	11% (2/18)	29% (4/14)	75% (6/8)
pTDP43	22% (4/18)	29% (4/14)	75% (6/8)
p value, C9 vs. nonC9			
H&E	< 0.005*	< 0.001*	0.10
pTDP43	< 0.001*	< 0.001*	0.515
p value, C9 vs. Control			
H&E	< 0.001*	< 0.001*	0.487
pTDP43	< 0.002*	< 0.001*	0.487

() Indicates the number of cases with granulo-vacuolar degeneration/the number of cases studied. *Fisher's exact test, significance level < 0.016 after Bonferroni correction

Table 5 Prevalence of GVD according to Braak's NFT stages

	Braak 0	Braak 1	Braak 2	Braak 3
FTLD/ALS-C9				
H&E	80% (8/10)	92% (12/13)	100% (3/3)	100% (3/3)
pTDP43	80% (8/10)	100% (13/13)	100% (3/3)	100% (3/3)
FTLD/ALS-nonC9				
H&E	20% (4/20)	35% (7/20)	50% (2/4)	100% (2/2)
pTDP43	20% (4/20)	45% (9/20)	75% (3/4)	100% (2/2)
Control				
H&E	7% (1/15)	14% (2/14)	71% (5/7)	100% (4/4)
pTDP43	13% (2/15)	14% (2/14)	86% (6/7)	100% (4/4)
p value, C9 vs. nonC9*				
H&E	0.004*	0.001*	0.428	1
pTDP43	0.004*	0.002*	1	1
p value, C9 vs. Control*				
H&E	< 0.001*	< 0.001*	1	1
pTDP43	0.002*	< 0.001*	1	1

() Indicates the number of cases with granulo-vacuolar degeneration/the number of cases studied

*Fisher's exact test, significance level < 0.016 after Bonferroni correction

Immunohistochemical characteristics of GVD

Immunohistochemistry of CHMP2B, a marker of the multivesicular bodies, strongly labeled GVD granules (Fig. 2). The GVD granules were also immunopositive for CK1δ, AT-8, and pTDP-43 (Fig. 2). By contrast, anti-p62 antibody, a marker of ubiquitinated proteins and autophagosomes, did not label GVD granules (Fig. 2). Sense- and antisense-DPRi were found within GVD vacuoles and involved GVD granules (Fig. 2). The sense-DPRi, comprising poly-GA, poly-GP, and poly-GR, were significantly more prevalent in the GVD-containing neurons than in the GVD-negative neurons (Table 6). The antisense-DPRi, comprising poly-PR and poly-PA, were also observed in the GVD-containing neurons, although in too small numbers to permit statistics. In nine cases with C9orf72 mutations, inclusions with an aspect compatible with GVD were also found in the granule cells of the dentate gyrus (Fig. 2). These were composed of basophilic granules in vacuoles, which were immunopositive for CHMP2B, CK1δ, pTDP-43, and AT-8. These inclusions were not found in the FTLD/ALS-nonC9 and control groups.

Confocal microscopy

Double immunofluorescence revealed that CHMP2B-immunopositive GVD granules frequently coexisted with poly-GA inclusions in the neurons (Fig. 3). On triple immunofluorescence, the GVD granules labeled with CHMP2B and CK1δ were attached to the surface of a poly-GA or a poly-PR inclusion. Three-dimensional-reconstruction images also revealed that CHMP2B- and CK1δ-immunopositive granules were attached to the surface of poly-GA or poly-PR inclusion. The triple immunofluorescence also showed that the CHMP2B- and CK1δ-immunopositive granules were attached to a poly-GA inclusion in a dentate gyrus granule cell (Fig. 3). The GVD granules were immunolabeled with AT-8 or anti-pTDP-43 antibodies (Fig. 4).

Discussion

We found a significantly higher prevalence of GVD in FTLD/ALS cases carrying the C9orf72 mutation compared to FTLD/ALS-TDP cases without the C9orf72 mutation, or controls. The prevalence was still high when the statistics were computed according to clinical subgroups of FTD and ALS, Braak NFT stages, or ages at death. The CA2 sector was most vulnerable for GVD in the C9orf72-mutated cases, whereas the CA1 and the subiculum were the most common topography in the non-mutated cases and in the controls. Immunohistochemical analyses showed that neurons with GVD more frequently contained DPR inclusions than those without GVD in the C9orf72-mutated cases. At confocal microscopy, GVD granules were attached to the surface of DPR inclusions, an observation that suggested that DPR inclusions were located within GVD vacuoles and did not simply displace them. These results also indicated that GVD and DPR did not coexist in the neurons by chance, but probably shared a common pathogenesis. It is generally

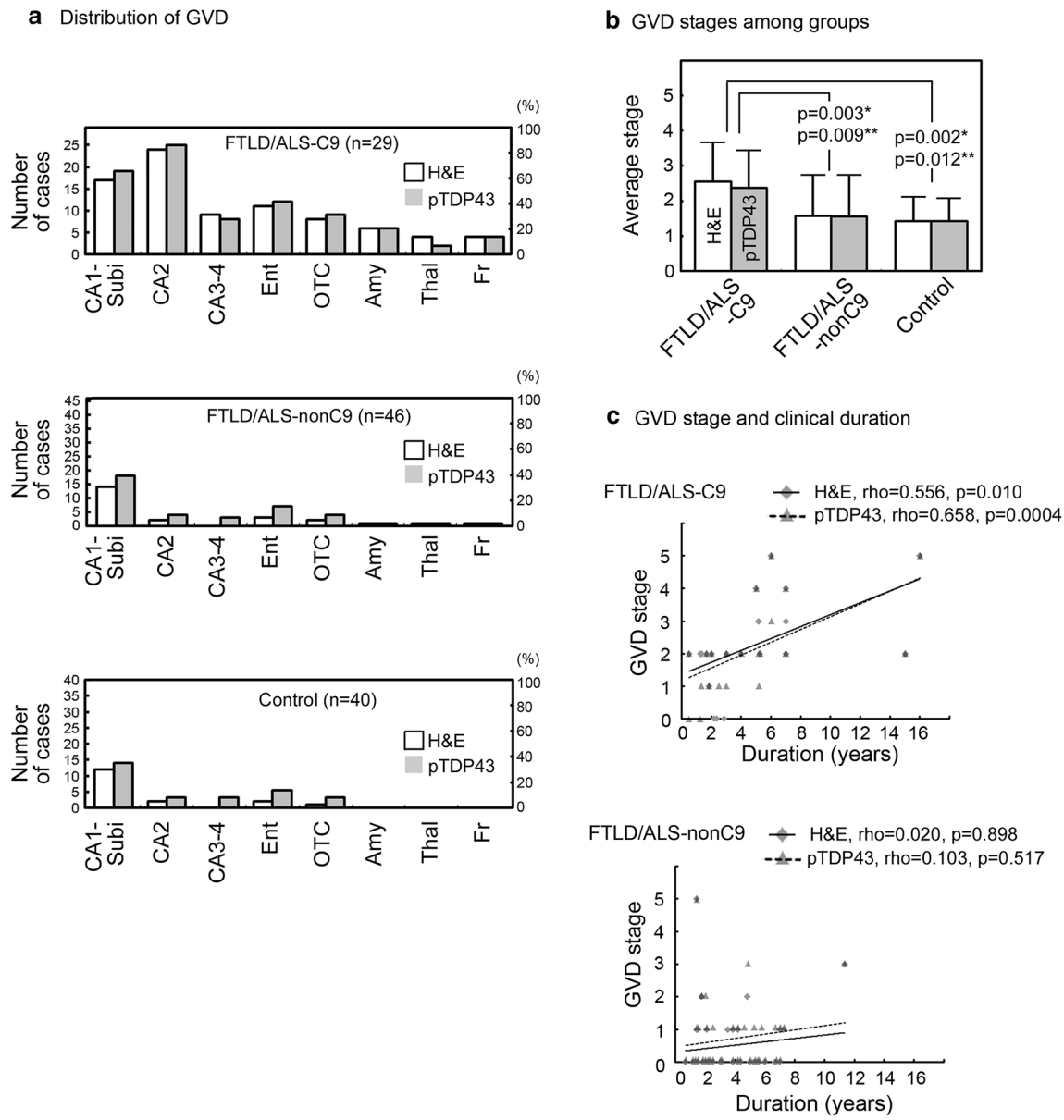

Fig. 1 Topographic distribution of GVD. **a** Prevalence of granulovacuolar degeneration (GVD) in various regions: CA1-subiculum (CA1-subi), CA2, CA3-4, entorhinal cortex (Ent), occipitotemporal cortex (OTC), amygdala (Amy), thalamus (Thal), and frontal cortex (Fr). For each group, the raw numbers and percentages of GVD-positive cases are indicated on the left and right scales, respectively. Counts have been performed after H&E staining (white columns) or anti-pTDP-43 immunohistochemistry (gray columns). In the FTLD/ALS-C9 group, GVD was most frequent in the CA2, followed by the CA1-subiculum. In the other groups, the CA1-subiculum was the most vulnerable. **b** Averages of GVD stages were compared among the GVD-positive individuals of each group. Stages of GVD were evaluated after H&E staining (white columns) or pTDP-43 immunohistochemistry (gray columns). Average GVD stage was higher in the FTLD/ALS-C9 group than in the other groups (Mann–Whitney *U* test with a Bonferroni correction). **c** The FTLD/ALS-C9 group showed a positive correlation between GVD stages and clinical durations (Spearman's rank correlation test, rho = 0.556 and $p < 0.005$ on H&E; rho = 0.658 and $p < 0.0005$ on pTDP-43). There was no correlation in the FTLD/ALS-nonC9 group

known that old age and NFTs are statistically linked with the density of GVD [11, 35, 39]. A previous study reported stages of GVD to be three or higher in a majority of AD cases [35]: GVD involves larger territories in AD cases than in C9orf72-mutated FTLD/ALS cases. However, the GVD stages were, on average, higher in C9orf72-mutated cases than in non-mutated FTLD/ALS cases; moreover, there was a positive correlation between GVD stages and disease durations. These results were also supportive of a pathophysiologic link between GVD formation and C9orf72 mutation. Another study has suggested that GVD granules were colocalized with components of the stress granules and

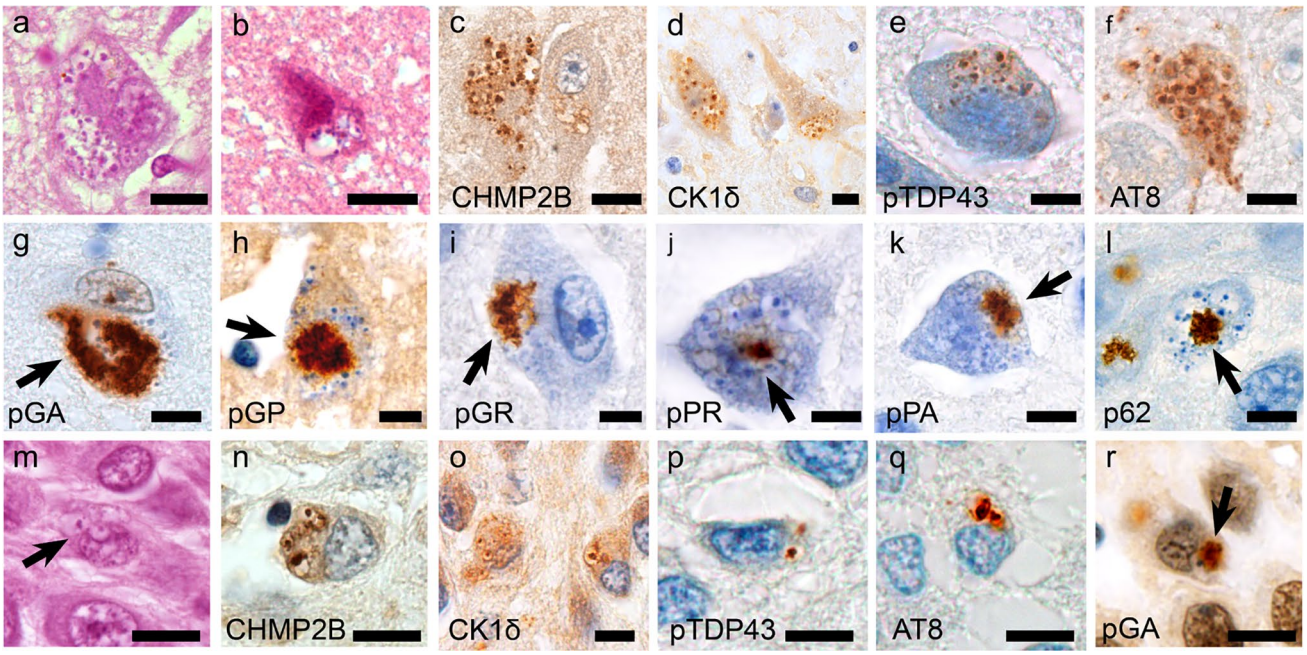

Fig. 2 GVD in FTLD/ALS-TDP cases with a C9orf72 mutation. Granulo-vacuolar degeneration (GVD) in CA2 (**a**) and in the frontal cortex (**b**). GVD granules were immunopositive for CHMP2B (**c**), CK1δ (**d**), phosphorylated TDP-43 (**e**), and AT-8 (**f**). DPR inclusions were labeled with poly-GA (**g** arrow), poly-GP (**h** arrow), poly-GR (**i** arrow), poly-PR (**j** arrow), and poly-PA (**k** arrow) antibodies; the inclusions were observed within GVD lesions. Anti-p62 immunohistochemistry was negative for GVD granules, whereas a coexisting DPR inclusion was immunopositive (**l** arrow). The dentate gyrus granule cells also demonstrated basophilic inclusions in vacuoles, compatible with GVD (**m** arrow). They were also immunopositive for CHMP2B (**n**), CK1δ (**o**), phosphorylated TDP-43 (**p**), and AT-8 (**q**). This change was associated with poly-GA inclusions (**r** arrow). Scale bars 10 µm. The pictures were taken in CA2 (**a**, **c**–**j**, **l**), CA1 (**k**), middle frontal cortex (**b**), and hippocampal granule cells (**m**–**r**)

Table 6 Occurrence of DPR inclusion in GVD-positive neurons

	GVD-positive neuron				GVD-negative neuron		Chi-square*	*p* value*
	Total count	Prevalence (SD)	Colocalize (%)	Differential (%)	Total count	Prevalence (SD)		
pGA inclusion								
CA1	42	67% ± 32.0	55	12	1085	21% ± 8.9	46.7	< 0.0001
CA2	41	76% ± 14.4	61	15	694	29% ± 9.7	39.66	< 0.0001
pGP inclusion								
CA1	46	43% ± 26.5	30	13	1005	12% ± 5.1	37.98	< 0.0001
CA2	38	37% ± 19.4	29	8	662	15% ± 4.8	13.19	< 0.0005
pGR inclusion								
CA1	39	38% ± 39.2	28	10	1178	10% ± 5.4	30.24	< 0.0001
CA2	30	37% ± 20.2	30	7	711	16% ± 3.1	9.278	< 0.005
pPR inclusion								
CA1	38	2.6% ± 9.3	2.6	0.0	1023	0.7% ± 0.6	NA**	NA**

Nine cases that showed granulo-vacuolar degeneration (GVD) both in the CA1 and CA2 sectors, and had both sense and antisense dipeptide repeat (DPR) inclusions were evaluated

*Chi-square test was performed between prevalence of dipeptide inclusion in GVD-positive and GVD-negative neurons. **NA, not assessed because of too small numbers of inclusions

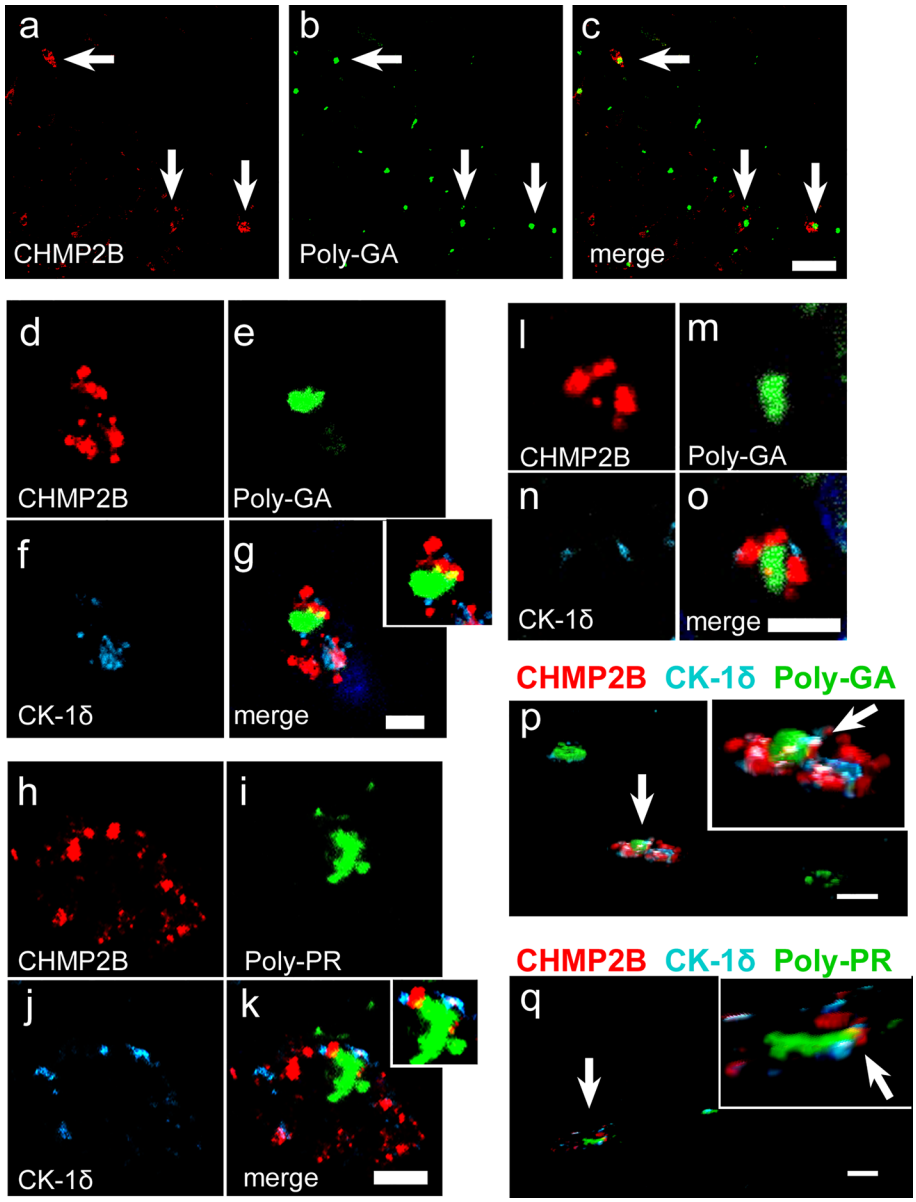

Fig. 3 GVD and DPR inclusion. **a–c** Neurons with granulovacuolar degeneration (GVD), labeled with CHMP2B antibody (red) frequently contained poly-GA cytoplasmic inclusions (green) in CA1 (arrows). **d–g** GVD granules labeled with CHMP2B and CK-1δ were attached to the surface of a poly-GA inclusion in a neuron of CA2. **h–k** The GVD granules were attached to a poly-PR inclusion in a neuron of CA2. **l–o** CHMP2B- and CK-1δ-immunopositive granules were attached to a poly-GA inclusion within a dentate gyrus granule cell. **p**, **q** A 3-dimensional reconstruction also revealed that CHMP2B- and CK-1δ-immunopositive GVD granules were attached to the surface of a poly-GA or poly-PR inclusion. Scale bars **a–c** 50 µm and **d–q** 10 µm

could be a neuroprotective reaction against oxidative stress [6]. GVD has been found in ganglion cell tumors from cases under 30 years of age [4, 24]. These reports and our results indicate that NFTs and aging are not the single determinants of GVD formation.

In previous studies, pTau has also been used to label GVD granules with a high sensitivity [11]. We chose, however, to resort to conservative H&E and anti-pTDP-43 immunohistochemistry that avoided overestimating the prevalence of the lesions and the possible interference of cytoplasmic tau pathology. Immunohistochemical characteristics of GVD observed in C9orf72-mutated cases were similar to those of GVD described in AD cases and elderly individuals. We also found CHMP2B-, CK1δ-, pTau-, and pTDP-43-positive inclusions consistent with GVD in the dentate gyrus granule cells of cases with C9ORF72 mutations. This topography is not their usual location [35] and could be specific to this mutation.

Although the mechanism for GVD formation in the C9ORF72 mutation is uncertain, we found DPR-positive inclusions, at least those derived from sense translation, to be frequent in GVD-containing neurons. Sense DPRi were more frequent than antisense DPRi as already noticed [15]. The coexistence of DPR-positive inclusions and GVD in the neurons suggests that the C9ORF72 mutation facilitates the formation of GVD. Several studies have revealed a similarity between GVD granules and the autophagic organelle, indicating that GVD reflects a perturbation of certain steps in the autophagy system and a failure to complete lysosome formation [9, 39]. Although the initial components of the

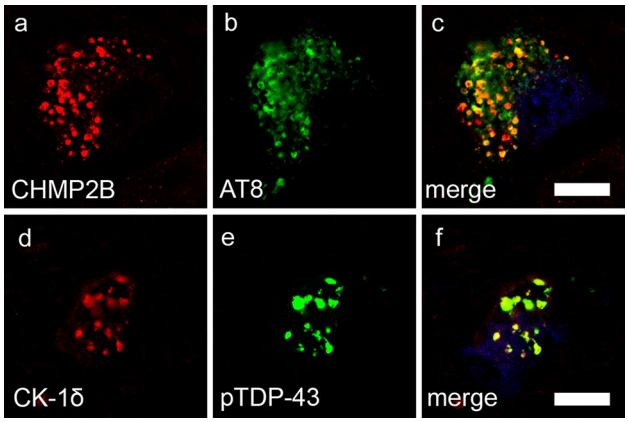

Fig. 4 Immunoreactivity of AT-8 and pTDP-43 in GVD granules. Signals of AT-8 (**a**–**c**) or anti-phosphorylated TDP-43 (**d**–**f**) immunohistochemistry were merged with GVD granules labeled with CHMP2B or CK-1δ in CA2 neurons. Scale bars 10 µm

autophagy system are the endosome and autophagosome [25], CHMP2B, a subunit of ESCRT-III endosomal trafficking machinery, was abundant in GVD granules [9, 39]. By contrast, p62 and LC3, which are expressed in autophagosomes, were sparse in GVD granules [9]. The C9orf72 mutation has recently been shown to induce haploinsufficiency that impairs endosomal trafficking, which results in reduced lysosomal generation and low clearance of DPR inclusions [31]. It is likely that a disruption of endosome formation, related to the C9orf72 mutation, contributes to GVD formation.

DPR inclusions were abundant in the cerebellum of C9orf72-mutated cases, but GVD was not seen in that location. This observation indicates that the interaction between the formation of DPR inclusions and GVD depends on multiple factors. A similar observation may be made concerning the relationship between pTau and GVD; pTau accumulates in the locus coeruleus during the early phase of AD [3], although GVD is usually absent. The formation of GVD might require not only the presence of aggregated protein but also other factors depending on the metabolism, activity, or types of involved neurons.

In conclusion, we found an unexpectedly high prevalence of GVD in C9orf72-related FTLD/ALS-TDP cases compared to non-C9orf72 FTLD/ALS-TDP cases and neurologically normal individuals of the same age. GVD progressed more extensively during the disease course in C9orf72-mutated cases. DPR inclusions were more frequently found in GVD-containing neurons than in neurons devoid of them. The C9orf72 mutation causing a deficit in the endosomal pathway may facilitate the development of GVD.

Acknowledgements This study is supported by Grants for aid from Uehara Memorial Foundation, Kanae Foundation for the Promotion of Medical Science, and Mochida Memorial Foundation for Medical and Pharmacological Research. The NeuroCEB Brainbank is funded by the patient associations ARSEP (multiple sclerosis), CSC (Connaître les Syndromes Cérébelleux), France Alzheimer, France Parkinson, ARSLA (Association pour la recherche sur la SLA), France DFT (Dégénérescence Fronto-Temporale), and CADASIL France. We also give special thanks to the technicians of the Department of Neuropathology, Pitié-Salpêtrière Hospital. Members of the NeuroCEB Brainbank Neuropathology Network: Letournel F, Martin-Négrier M-L, Chapon F, Godfraind C, Maurage C-A, Deramecourt V, Meyronet D, Streichenberger N, Maues de Paula A, Rigau V, Vandenbos-Burel F, Milin S, Chiforeanu DC, Laquerrière A, and Lannes B.

Author contributions Study concept: YR, DS, and CD; pathologic data acquisition: YR and DS; clinical data acquisition: FS, IL; genetic tests: SM, IL; autopsy, and tissue archive: SB, IP, DS, and CD; technical instructions: MY, GS, TA, and MK; drafting manuscript: YR; supervisor: DS and CD.

Compliance with ethical standards

Conflict of interest The authors declare that they have no competing interest.

References

1. Al-Sarraj S, King A, Troakes C, Smith B, Maekawa S, Bodi I et al (2011) p62 positive, TDP-43 negative, neuronal cytoplasmic and intranuclear inclusions in the cerebellum and hippocampus define the pathology of C9orf72-linked FTLD and MND/ALS. Acta Neuropathol 122:691–702
2. Braak H, Alafuzoff I, Arzberger T, Kretzschmar H, Del Tredici K (2006) Staging of Alzheimer disease-associated neurofibrillary pathology using paraffin sections and immunocytochemistry. Acta Neuropathol 112:389–404
3. Braak H, Thal DR, Ghebremedhin E, Del Tredici K (2011) Stages of the pathologic process in Alzheimer disease: age categories from 1 to 100 years. J Neuropathol Exp Neurol 70:960–969
4. Brat DJ, Gearing M, Goldthwaite PT, Wainer BH, Burger PC (2001) Tau-associated neuropathology in ganglion cell tumours increases with patient age but appears unrelated to ApoE genotype. Neuropathol Appl Neurobiol 27:197–205
5. Brooks BR, Miller RG, Swash M, Munsat TL, World Federation of Neurology Research Group on Motor Neuron Diseases (2000) El Escorial revisited: revised criteria for the diagnosis of amyotrophic lateral sclerosis. Amyotroph Lateral Scler Other Motor Neuron Disord 1:293–299
6. Castellani RJ, Gupta Y, Sheng B, Siedlak SL, Harris PL, Coller JM et al (2011) A novel origin for granulovacuolar degeneration in aging and Alzheimer's disease: parallels to stress granules. Lab Invest 91:1777–1786
7. Davidson Y, Robinson AC, Liu X, Wu D, Troakes C, Rollinson S et al (2016) Neurodegeneration in frontotemporal lobar degeneration and motor neurone disease associated with expansions in C9orf72 is linked to TDP-43 pathology and not associated with aggregated forms of dipeptide repeat proteins. Neuropathol Appl Neurobiol 42:242–254
8. DeJesus-Hernandez M, Mackenzie IR, Boeve BF, Boxer AL, Baker M, Rutherford NJ et al (2011) Expanded GGGGCC hexanucleotide repeat in noncoding region of C9ORF72 causes chromosome 9p-linked FTD and ALS. Neuron 72:245–256

9. Funk KE, Mrak RE, Kuret J (2011) Granulovacuolar degeneration (GVD) bodies of Alzheimer's disease (AD) resemble late-stage autophagic organelles. Neuropathol Appl Neurobiol 37:295–306
10. Geser F, Martinez-Lage M, Robinson J, Uryu K, Neumann M, Brandmeir NJ et al (2009) Clinical and pathological continuum of multisystem TDP-43 proteinopathies. Arch Neurol 66:180–189
11. Hunter S, Minett T, Polvikoski T, Mukaetova-Ladinska E, Brayne C, Cambridge City over-75s Cohort Collaboration (2015) Re-examining tau-immunoreactive pathology in the population: granulovacuolar degeneration and neurofibrillary tangles. Alzheimers Res Ther 7:57
12. Ince PG, Lowe J, Shaw PJ (1998) Amyotrophic lateral sclerosis: current issues in classification, pathogenesis and molecular pathology. Neuropathol Appl Neurobiol 24:104–117
13. Kadokura A, Yamazaki T, Kakuda S, Makioka K, Lemere CA, Fujita Y et al (2009) Phosphorylation-dependent TDP-43 antibody detects intraneuronal dot-like structures showing morphological characters of granulovacuolar degeneration. Neurosci Lett 463:87–92
14. Köhler C (2016) Granulovacuolar degeneration: a neurodegenerative change that accompanies tau pathology. Acta Neuropathol 132:339–359
15. Mackenzie IR, Frick P, Grässer FA, Gendron TF, Petrucelli L, Cashman NR (2015) Quantitative analysis and clinico-pathological correlations of different dipeptide repeat protein pathologies in C9ORF72mutation carriers. Acta Neuropathol 130:845–861
16. Mackenzie IR, Neumann M, Baborie A, Sampathu DM, Du Plessis D, Jaros E et al (2011) A harmonized classification system for FTLD-TDP pathology. Acta Neuropathol 122:111–113
17. May S, Hornburg D, Schludi MH, Arzberger T, Rentzsch K, Schwenk BM et al (2014) C9orf72 FTLD/ALS-associated Gly-Ala dipeptide repeat proteins cause neuronal toxicity and Unc119 sequestration. Acta Neuropathol 128:485–503
18. McKeith IG, Boeve BF, Dickson DW, Halliday G, Taylor JP, Weintraub D et al (2017) Diagnosis and management of dementia with Lewy bodies: fourth consensus report of the DLB Consortium. Neurology 89:88–100
19. Millecamps S, Boillee S, Le Ber I, Seilhean D, Teyssou E, Giraudeau M et al (2012) Phenotype difference between ALS patients with expanded repeats in C9ORF72 and patients with mutations in other ALS-related genes. J Med Genet 49:258–263
20. Mori K, Weng SM, Arzberger T, May S, Rentzsch K, Kremmer E et al (2013) The C9orf72 GGGGCC repeat is translated into aggregating dipeptide-repeat proteins in FTLD/ALS. Science 339:1335–1338
21. Murray ME, DeJesus-Hernandez M, Rutherford NJ, Baker M, Duara R, Graff-Radford NR et al (2011) Clinical and neuropathologic heterogeneity of c9FTD/ALS associated with hexanucleotide repeat expansion in C9ORF72. Acta Neuropathol 122:673–690
22. Neary D, SnowdenJS Gustafson L, Passant U, Stuss D, Black S et al (1998) Frontotemporal lobar degeneration: a consensus on clinical diagnostic criteria. Neurology 51:1546–1554
23. Neumann M, Sampathu DM, Kwong LK, Truax AC, Micsenyi MC, Chou TT et al (2006) Ubiquitinated TDP-43 in frontotemporal lobar degeneration and amyotrophic lateral sclerosis. Science 314:130–133
24. Prabowo AS, Iyer AM, Veersema TJ, Anink JJ, Schouten-van Meeteren AY, Spliet WG et al (2015) Expression of neurodegenerative disease-related proteins and caspase-3 in glioneuronal tumours. Neuropathol Appl Neurobiol 41:e1–e15
25. Raiborg C, Stenmark H (2009) The ESCRT machinery in endosomal sorting of ubiquitylated membrane proteins. Nature 458:445–452
26. Riku Y, Watanabe H, Yoshida M, Mimuro M, Iwasaki Y, Masuda M et al (2017) Pathologic involvement of glutamatergic striatal inputs from the cortices in TAR DNA-binding protein 43 kDa-related frontotemporal lobar degeneration and amyotrophic lateral sclerosis. J Neuropathol Exp Neurol 76:759–768
27. Riku Y, Watanabe H, Yoshida M, Mimuro M, Iwasaki Y, Masuda M et al (2016) Marked involvement of the striatal efferent system in TAR DNA-binding protein 43 kDa-related frontotemporal lobar degeneration and amyotrophic lateral sclerosis. J Neuropathol Exp Neurol 75:801–811
28. Riku Y, Watanabe H, Yoshida M, Tatsumi S, Mimuro M, Iwasaki Y et al (2014) Lower motor neuron involvement in TAR DNA-binding protein of 43 kDa-related frontotemporal lobar degeneration and amyotrophic lateral sclerosis. JAMA Neurol 71:172–179
29. Saito Y, Ruberu NN, Sawabe M, Arai T, Tanaka N, Kakuta Y et al (2004) Staging of argyrophilic grains: an age-associated tauopathy. J Neuropathol Exp Neurol 63:911–918
30. Seilhean D, Le Ber I, Sarazin M, Lacomblez L, Millecamps S, Salachas F et al (2011) Fronto-temporal lobar degeneration: neuropathology in 60 cases. J Neural Transm (Vienna) 118:753–764
31. Shi Y, Lin S, Staats KA, Li Y, Chang WH, Hung ST et al (2018) Haploinsufficiency leads to neurodegeneration in C9ORF72 ALS/FTD human induced motor neurons. Nat Med 24:313–325
32. Sullivan PM, Zhou X, Robins AM, Paushter DH, Kim D, Smolka MB et al (2016) The ALS/FTLD associated protein C9orf72 associates with SMCR32 and WDR41 to regulate the autophagy-lysosome pathway. Acta Neuropathol Commun 4:51
33. Swinnen B, Bento-Abreu A, Gendron TF, Boeynaems S, Bogaert E, Nuyts R et al (2018) A zebrafish model for C9orf72 ALS reveals RNA toxicity as a pathogenic mechanism. Acta Neuropathol 135:427–443
34. Takeda T, Seilhean D, Le Ber I, Millecamps S, Sazdovitch V, Kitagawa K et al (2017) Amygdala TDP-43 pathology in frontotemporal lobar degeneration and motor neuron disease. J Neuropathol Exp Neurol 76:800–812
35. Thal DR, Del Tredici K, Ludolph AC, Hoozemans JJ, Rozemuller AJ, Braak H et al (2011) Stages of granulovacuolar degeneration: their relation to Alzheimer's disease and chronic stress response. Acta Neuropathol 122:577–589
36. Thal DR, Rüb U, Orantes M, Braak H (2002) Phases of A beta-deposition in the human brain and its relevance for the development of AD. Neurology 58:1791–1800
37. Vatsavayai SC, Yoon SJ, Gardner RC, Gendron TF, Vargas JN, Trujillo A et al (2016) Timing and significance of pathological features in C9orf72 expansion-associated frontotemporal dementia. Brain 39:3202–3216
38. Yamazaki Y, Matsubara T, Takahashi T, Kurashige T, Dohi E, Hiji M et al (2011) Granulovacuolar degenerations appear in relation to hippocampal phosphorylated tau accumulation in various neurodegenerative disorders. PLoS One 6:e26996
39. Yamazaki Y, Takahashi T, Hiji M, Kurashige T, Izumi Y, Yamawaki T et al (2010) Immunopositivity for ESCRT-III subunit CHMP2B in granulovacuolar degeneration of neurons in the Alzheimer's disease hippocampus. Neurosci Lett 477:86–90